Molecular Crystals and Liquid Crystals
Publication details, including instructions for authors and subscription information:
http://www.tandfonline.com/loi/gmcl20

Ab Initio Study of ^{2}H Nuclear Quadrupole Coupling Constants in Deuterated Crystalline Oxalic Acid Dehydrated Polymorphs

Cuauhtémoc Samaniego [a], J. G. Rodríguez-Zavala [b], F. J. Tenorio [b] & R. Flores-Moreno [c]

[a] College of Engineering and Technology, The American University of the Middle East, Dasman, Kuwait

[b] Departamento de Ciencias Exactas y Tecnologías, Centro Universitario de Los Lagos, Universidad de Guadalajara, Lagos de Moreno, Jalisco, México

[c] Departamento de Química Centro Universitario de Ciencias Exactas e Ingenierías, Universidad de Guadalajara Blvd., Marcelino García Barragán Guadalajara, Jalisco, México

Published online: 22 Apr 2013.

To cite this article: Cuauhtémoc Samaniego, J. G. Rodríguez-Zavala, F. J. Tenorio & R. Flores-Moreno (2013) Ab Initio Study of ^{2}H Nuclear Quadrupole Coupling Constants in Deuterated Crystalline Oxalic Acid Dehydrated Polymorphs, Molecular Crystals and Liquid Crystals, 575:1, 188-201, DOI: 10.1080/15421406.2013.768500

To link to this article: http://dx.doi.org/10.1080/15421406.2013.768500

Mol. Cryst. Liq. Cryst., Vol. 575: pp. 188–201, 2013

ISSN: 1542-1406 print/1563-5287 online
DOI: 10.1080/15421406.2013.768500

Ab Initio Study of ^{2}H Nuclear Quadrupole Coupling Constants in Deuterated Crystalline Oxalic Acid Dehydrated Polymorphs

CUAUHTÉMOC SAMANIEGO,[1,*]
J. G. RODRÍGUEZ-ZAVALA,[2] F. J. TENORIO,[2]
AND R. FLORES-MORENO[3]

[1]College of Engineering and Technology, The American University of the Middle East, Dasman, Kuwait
[2]Departamento de Ciencias Exactas y Tecnologías, Centro Universitario de Los Lagos, Universidad de Guadalajara, Lagos de Moreno, Jalisco, México
[3]Departamento de Química Centro Universitario de Ciencias Exactas e Ingenierías, Universidad de Guadalajara Blvd., Marcelino García Barragán Guadalajara, Jalisco, México

We report calculated ^{2}H nuclear quadrupole coupling constants and asymmetry parameter in deuterated crystalline oxalic acid dihydrated polymorphs within a full-potential linear combination of Gaussian-type orbitals employing both Density Functional Theory and Hartree-Fock approximation. The Becke's hybrid exchange B3 and the Lee, Yang and Parr correlation functionals were employed. Their dependence with basis set, interelectronic correlation, structural changes and crystal field environment are reported.

Keywords Molecular crystals; Nuclear quadrupole coupling constants; Polymorphs

1. Introduction

Currently, periodic ab initio methods enable high quality to be extended to crystalline solids and open new possibilities to investigate properties affected by the long-range periodic environment. Particularly, molecular crystals are suitable prototype systems that allow the influence of the crystal environment to be quantified, since they display a clear separation of the intramolecular (short) and intermolecular (large) contributions for relevant molecular properties [1–21].

Some 74% of nuclear magnetic resonance (NMR) active nuclei have a spin (I) bigger than $\frac{1}{2}$, and so possessing a nuclear electric quadrupole moment (NQM) [22,23] that enable them to interact with any electric field gradient (EFG) at the atomic nucleus. The nuclear quadrupole coupling constant (NQCC) represents the strength of such interaction.

Theoretically, the electric field gradient (EFG) defined as the second derivative of the electrostatic potential at an atomic nucleus clearly depends on the distribution of charge

*Address correspondence to Cuauhtémoc Samaniego, College of Engineering and Technology, The American University of the Middle East, P.O. BOX 220, Dasman, 15453 Kuwait. Tel.: +96 52 2251400 x 1261; Fax: +96 52 2251427. E-mail: jose.reyna@aum.edu.kw

around the nucleus which can be determined directly from the knowledge of the electronic wave function and arises naturally in molecules and crystalline solids by virtue of other nuclei and electrons in their vicinity [24].

Experimentally, NQCC can be measured with high precision from microwave and Mossbaüer spectroscopy for gaseous molecules, or from nuclear quadrupole resonance spectroscopy, from the splitting of nuclear magnetic resonance spectra and from X-ray diffraction data in crystalline solids [23–25].

Previous periodic ab initio studies of NQCCs on molecular crystals have been mainly concerned with the determination of NQCCs at the heavy (e.g., nitrogen and oxygen) nuclei and only a few have been dedicated to the evaluation of Deuterium Quadrupole Coupling Constant (DQCC) [26–33].

Camus et al. [26], properly selected the oxalic acid molecule in the α and β phases of oxalic acid dihydrate ($C_2D_2O_4 \cdot 2D_2O$) as the prototype system in order to explore the level of the computational approach required to yield high quality prediction of experimental DQCCs and to quantify the influence of the crystal environment. Camus et.al. calculated DQCCs at the periodic Hartree-Fock level of theory, employing the 6-21G** and 6-31G** basis. They investigated the correlations between the calculated DQCCs and geometrical parameters. Moreover, results demonstrate the importance of considering the full periodic structure. In the previous study, convergence problems due to basis set linear dependence were reported for the α phase at low temperature (100 K and 15 K) using the 6-31G** basis set. To circumvent this, the orbital exponents were scaled by 1.01 and 1.02. For proper comparison, the low temperature DQCCs for the α phase were obtained by linear extrapolation with scaling factor 1.00. For the asymmetry parameter (η), scaling and extrapolation may be critical as small errors in the calculated values of the electric field gradient components are amplified when taking differences and ratios, and therefore can lead to the propagation of significant errors.

In order to quantify the influence of the crystal environment and also to test the accuracy of the computational approach employed, both the structural information determined from neutron diffraction data which provides accurate positions of the ^2H nuclei [34,35], and the experimental DQCCs are available for two crystalline phases (α and β) of deuterated oxalic acid dihydrate($C_2D_2O_4 \cdot 2D_2O$) [36].

This work presents both ab initio periodic Hartree-Fock and Density Functional calculations of DQCC for the oxalic acid molecule in the α and β phase of deuterated crystalline oxalic acid dihydrate. The role of basis sets, electronic correlation, structural changes, and crystal field contributions are mainly discussed.

2. Structural Details

Deuterated oxalic acid dihydrate ($C_2D_2O_4 \cdot 2D_2O$) presents two crystalline polymorphs (α and β phases). The α phase (space group $P2_{1/n, z=2}$, see Fig. 1(a)) has been determined by neutron diffraction at [15 K] $a = 6.137$Å, $b = 3.475$ Å, $c = 11.970$ Å, $\gamma = 105.978$; [100 K] $a = 6.133$ Å, $b = 3.500$ Å, $c = 11.983$ Å, $\gamma = 106.060$ and [298 K] $a = 6.150$ Å, $b = 3.605$ Å, $c = 12.102$ Å, $\gamma = 106.63$ [34,35]. The β phase (space group $P21/a$, $z = 2$, see Fig. 2(b)) has been determined by neutron diffraction at [298 K] $a = 10.021$ Å, $b = 5.052$ Å, $c = 5.148$ Å, $\gamma = 99.270$ [35].

The oxalic acid molecule ($C_2D_2O_4$) is planar and center-symmetric in both crystal phases. The molecule is hydrogen bonded to two equivalent pairs of D_2O molecules (see Fig. 3). Considering the neutron diffraction data measured at 298 K, the oxalic acid

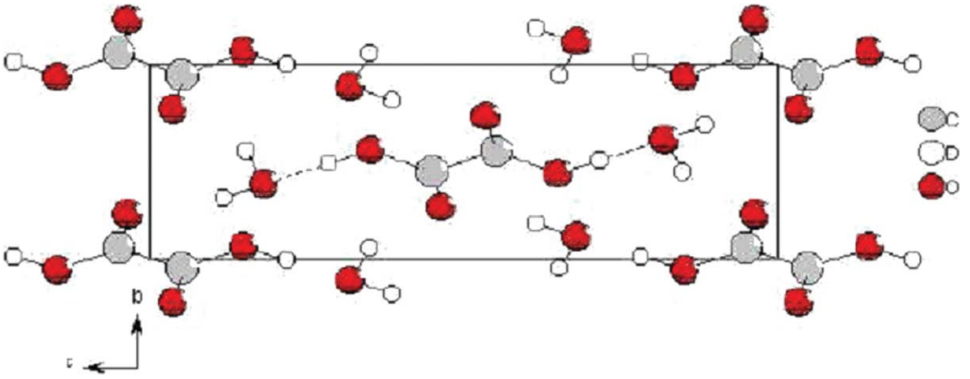

Figure 1. (a) The crystal structure of α phase of deuterated oxalic acid dihydrate.

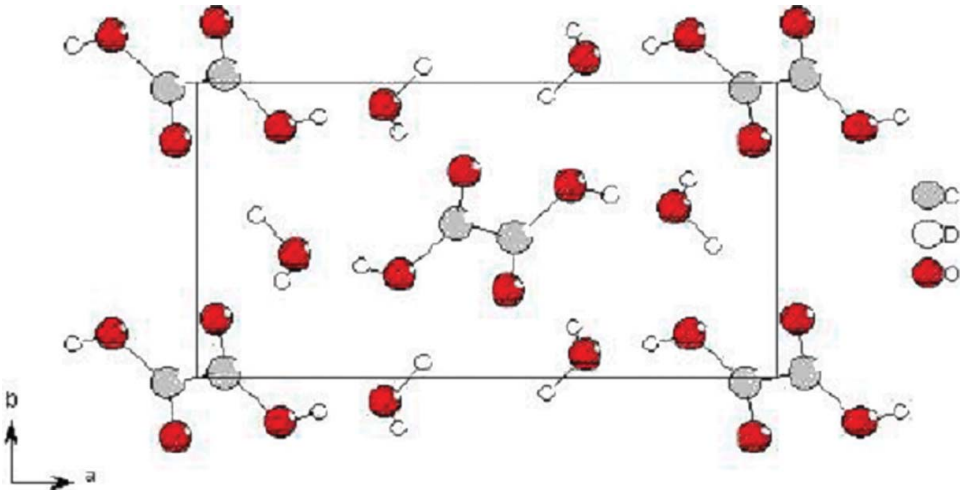

Figure 2. (b) The crystal structure of β phase of deuterated oxalic acid dihydrate.

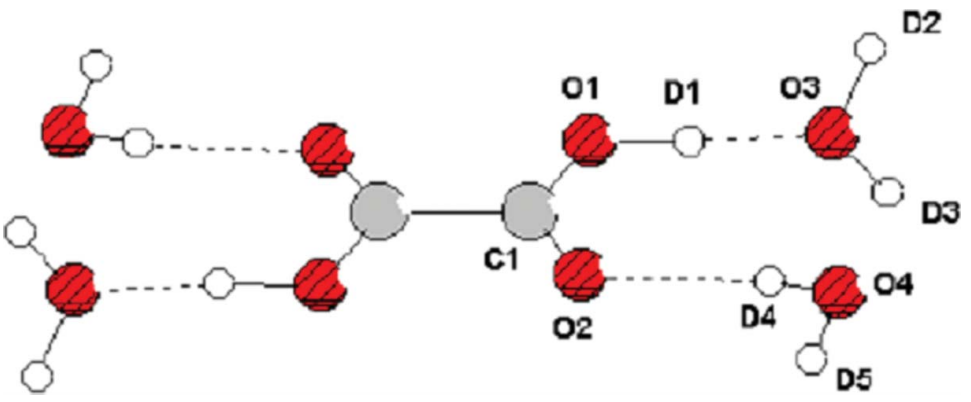

Figure 3. The oxalic acid molecule and four of the water molecules to which it is hydrogen bonded.

O_1-D_1 bond length is 1.030 Å and 1.020 Å, in the α and β phases, respectively, whereas the hydrogen bond length D1···O3 is 1.493 Å (α) and 1.520°A (β). The oxalic acid $C_1=O_2$ bond length is 1.207°A (α) and 1.203°A, (β) and the hydrogen bond length $D_4\cdots O_2$ is 2.007°A (α) and 1.960°A (β).

The hydrogen bond angle ($O_1-D_1\cdots O_3$) is close to linear in both phases: approximately 175.5° (α) and 174.2° (β). The hydrogen bond angle ($C_1 = O_2\cdots D_4$) is 129.6° (α) and 132.8° (β). The bond angles ($D_2-O_3\cdots D_1$) and ($D_3-O_3\cdots D_1$) are 113.7° and 119.4° for the α phase and 119.8° and 131.4° for the β phase. The bond angles ($O_4-D_4\cdots O_2$) and ($O_4-D_5\cdots O_2$) are 156.0° and 70.3° for the α phase and 157.34° and 67.7° for the β phase. The torsion angles are defined as $\varphi_1(O_1-D_1\cdots O_3-D_2)$, $\varphi_2(O_1-D_1\cdots O_3-D_3)$, $\varphi_3(C_1-O_2\cdots D_4-O_4)$, and $\varphi_4(C_1-O_2\cdots D_5-O_4)$. The values of these torsion angles (φ_1, φ_2, φ_3, φ_4) for the α and β phases are: [α] ($\pm$9.6°, $\pm$135.5°, $\pm$153.4°, 0°); [β]($\pm$65.9°, $\pm$112.0°, $\pm$161.3°, $\pm$2.3°).

Throughout this study, calculations are performed on deuterated samples. In neutron diffraction experiments, deuterium atoms have enhanced scattering amplitudes, reduced thermal mean square displacement amplitudes, and the absorption and incoherent background problem that arises with hydrogen is eliminated. This results in more accurate geometry information.

3. Quadrupole Coupling Constants

The electric field gradient at the nucleus is described by a second rank tensor V, and clearly depends on the distribution of charge around the nucleus. Theoretically, the charge distribution (and hence V) may be determined directly from knowledge of the electronic wavefunction and the nuclear positions for the system of interest.

For any arbitrary distribution of the electric charge, there exists a principal axis system (V^{PAS}) in which the off-diagonal EFG tensor elements are zero. The V^{PAS} tensor is thus diagonal; it is also traceless (i.e., $V_{zz} = -[V_{xx} + V_{yy}]$) and, therefore, there are only two independent principal components. The axes are chosen such that $|V_{zz}|\geq|V_{yy}|\geq|V_{xx}|$. The quantities commonly used to describe the tensor in crystals are: first, the nuclear quadrupole coupling constant (NQCC) which is directly proportional to both the principal component with largest magnitude (V_{zz}) and the nuclear quadrupole moment (NQM) of the nucleus (Eq. 1). Second, the asymmetry parameter (η) that is a measure of the deviation of the electric field from the cylindrical symmetry (Equation 2), it lies in the range $0 \leq \eta \leq 1$, with $\eta = 0$ in the case of axial symmetry.

$$\mathrm{DQCC} = (e/h)(\mathrm{NQM})\, V_{zz}, \tag{1}$$

$$\eta = (|V_{xx}| - |Vyy|)/|V_{zz}|. \tag{2}$$

For the O_1-D_1 bond in the oxalic acid molecule (see Fig. 3), the z-axis of V^{PAS} for the ^{2}H nuclei lies close to the direction of the bond and although not possessing axial symmetry the value of η is usually fairly close to zero. DQCCs have been measured and reported by solid-state deuterium nuclear magnetic resonance spectroscopy for both the α and β phases of crystalline oxalic acid dihydrate at 298 K [36].

4. Computational Methodology

The CRYSTAL09 program was used to carry out all single points calculations at the experimentally determined crystal structures of the α and β phases of the deuterated

oxalic acid dihydrate, including those on isolated molecules at both Hartree-Fock (HF) and Density Functional Theory (DFT) [37]. The fundamental approximation is the expansion of symmetry adapted single particle wave functions as a linear combination of Bloch functions defined in terms of linear combinations of Gaussian type functions (GTF) [37]. The exchange-correlation effects are included by using the Becke's hybrid exchange B3 and the Lee, Yang, and Parr correlation functional (B3LYP) [38, 39].

This study has been focused on the DQCC and η values of the ^{2}H nucleus (D_1 in Fig. 3) of the oxalic acid molecule for the two distinct environments in the α and β phases of the deuterated oxalic acid dihydrate.

First, the DQCC (χ^{MOL}) and asymmetry parameter (η^{MOL}) have been calculated for an isolated oxalic acid molecule with the molecular geometry extracted from the relevant solids. Second, the DQCC (χ^{CLS}) and asymmetry parameter (η^{CLS}) have been calculated for a cluster extracted from the solids and composed of an oxalic acid molecule surrounded by four close neighboring water molecules (see Fig. 3). Third, the DQCC (χ^{LAT}) and asymmetry parameter (η^{LAT}) have been calculated for the periodic crystal structures. Fourth, $\chi^{DIF} = \chi^{MOL} - \chi^{CLS}$ defined as the contributions to the DQCC from the first shell of four neighboring water molecules have been calculated.

The following basis sets: 6-21G** [40], 6-31G** [41–43], and Thakkar double-zeta with polarization (DZP) [44] were investigated. For the atoms C and O, the 6-21G** basis set can be represented by (9s3p) primitive Gaussians contracted to [3s2p] via a {621/21} scheme, the 6-31G** basis being (10s4p) contracted to [3s2p] via a {631/31}scheme, while the DZP is (9s5p) contracted to [4s2p] via a {6211/41}for C and O. For atoms C and O, the *d* polarization functions exponents are the same for the 6-21G** and 6-31G** basis sets, namely $0.8a_0^{-1}$ for C and O [45]. For DZP basis the *d* polarization functions exponents are those labeled Pa in Table IX from Thakkar et al. [44].

For the H atom, the 6-21G** basis can be represented by (3s) primitive Gaussians contracted to [2s1s] via a {21} scheme. The 6-31G** and DZP basis sets use the same (4s) contracted to [3s1s] via a {31} scheme. The inner and outer exponents are both scaled by 1.10^2 for the 6-21G basis, 1.20^2 and 1.15^2, respectively, for the 6-31G basis set, and 1.20^2 in both cases for DZP. The s polarization functions exponents are the same for the 6-21G** and 6-31G** basis sets, 1.1 a_0^{-1} [45], and 1.0 a_0^{-1} for the DZP basis set (labeled Pa in Table IX from Thakkar et al. [44]).

In the DFT calculations, the exchange-correlation potential is expanded in an auxiliary basis set of Gaussian-type functions (GTF), with even tempered exponents. For atom H and atoms C and O, the expansion contains {s,p,d} and {s,p,d,f,g} GTFs, respectively. For the numerical integration, the atomic partition method proposed by Becke has been adopted [46].

The numerical values of parameters (ITOL1, ITOL2, ITOL3, ITOL4, ITOL5) controlling the evaluation of the Coulomb (for both HF and DFT) and Exchange terms (for HF) have been fixed to 8, 8, 8, 8, and 16, respectively, to ensure a high numerical accuracy, therefore, avoiding convergence problems due to basis set pseudolinear dependence previously reported by Camus et al. [26]. The number of reciprocal lattice points (*k* points) at which the Hamiltonian matrix has been diagonalized is 30 in both the α and β phases, corresponding to a shrinking factor of 4.

The CRYSTAL09 program gives EFGs in atomic units (1 a.u. $\equiv 9.7174 \times 10^{21}$ V m^2). The electric nuclear quadrupole moment (NQM) of ^{2}H nucleus was taken to be 2.86 mbarn (1 barn $\equiv 10^{-28}$ m^2) [23,24]. To obtain DQCCs in kHz, Equation 1 is given as: χ(kHz) = 234.96 $\times$ NQM (mbarn) $\times$ V_{zz}(a.u.).

5. Results and Discussion

Calculated single point HF and DFT-B3LYP values of DQCC and η for the α (15, 100, and 298 K) and β phase (298 K) of deuterated oxalic acid dihydrate with 6-21G**, 6-31G** and DZP basis sets are presented in Table 1 and Table 2, respectively. The tables also list the experimental DQCC (χ^{EXP}) and asymmetry parameter (η^{EXP}) values. These results display the dependence of DQCC and η values on basis set, electronic correlation, structural changes, and crystal field effects.

5.1 Basis Set Dependence

From Tables 1 and 2 one can see that the expansion of inner valence functions on passing from the 6-21G** to the 6-31G** basis sets, appreciable lowers $\chi^{MOL,}$ χ^{CLS}, and χ^{LAT} by up to 20% and increases the $\eta^{MOL,}$ η^{CLS}, and η^{LAT} by up to 30%. Comparing the DQCC values calculated in this study and those obtained by Camus et al. [26] at the HF level of theory, we observed that our DQCC values are slightly larger by approximately 2 kHz using the 6-31G** basis set. Small differences on DQCC values using the 6-31G** basis set are mainly due to different numerical values of the ITOL parameters.

Furthermore, the relaxation of the constrain between the exponents of the *s* and *p* valence functions on passing from the 6-31G** to the DZP basis set increases $\chi^{MOL,}$ χ^{CLS}, and χ^{LAT} by up to 7%, while making only a very small change to the asymmetry parameter $\eta^{MOL,}$ η^{CLS}, and η^{LAT} (lowering it by approximately 1%). We note that the DZP basis set provides great flexibility in the valence region, while retaining an excellent description of the atomic cores, all within a basis set slightly large than the 6-31G**. In order to test for the variations of the polarization (for atoms C, O, and H) and outer valence (for H atom) exponents observed on passing form 6-31G** to DZP basis set, we performed calculations for the α phase at 298 K, using the polarization and outer exponents from the 6-31G** basis set and transferred to the DZP basis set. We found that the DQCC values are smaller by approximately 1 kHz and the η values lowers by 0.5% which basically imply that no significant changes are observed by small variations of the polarization and outer valence exponents on going form 6-31G** to DZP basis set.

Figures 4(a), 4(b), and 5(a) also show graphically how DQCC and η values are very sensitive to the expansion of inner valence functions and less sensitive to the relaxation of the constraint between the exponents of the *s* and *p* valence functions.

In Tables 1 and 2, one can observe that the DQCC values calculated using 6-31G** basis set are in excellent agreement with experimental measurements for the crystals of oxalic acid dihydrate at 298 K.

5.2 Correlation Effects

Comparing Tables 1 and 2, one may see that the inclusion of electronic correlation at DFT-B3LYP level of theory generally increases the DQCC and significantly lowers the η values.

χ^{LAT} and χ^{CLS} values increase by up to 9%, but χ^{MOL} values do not change significantly ($\approx$1%) using the 6-21G** basis set, and remain unchanged for larger basis sets 6-31G** and DZP. Figures 4(a) and 4(b) clearly display these results. On the other hand, $\eta^{MOL,}$ η^{CLS}, and η^{LAT} values are appreciably lowered by ca. 25%–40%.

It is also interesting to see that practically the same χ^{LAT} values are obtained at both the HF level of theory using the DZP basis set and the DFT-B3LYP level of theory using

Table 1. Calculated DQCC (χ) and asymmetry parameter (η) for α and β phases of deuterated oxalic acid dihydrate at the HF level of theory

Phase	T [K]	d (O_1–D_1) [Å]	$d(D_1\cdots O_3)$ [Å]	χ^{EXP} [kHz]	η^{EXP}	Basis	χ^{MOL} [kHz]	η^{MOL}	χ^{CLS} [kHz]	η^{CLS}	χ^{LAT} [kHz]	η^{LAT}	χ^{DIF} [kHz]	η^{DIF}
α	15	1.045	1.447			6-21G**	205.2	0.094	137.4	0.107	126.0	0.141	67.8	0.013
						6-31G**	167.6	0.127	109.4	0.155	99.2	0.205	58.2	0.028
						DZP	174.4	0.126	116.8	0.153	107.0	0.200	57.6	0.027
α	100	1.039	1.455			6-21G**	212.0	0.091	144.6	0.102	133.2	0.134	67.4	0.011
						6-31G**	174.0	0.123	116.2	0.146	106.1	0.192	57.8	0.023
						DZP	181.3	0.122	124.2	0.145	114.4	0.187	57.1	0.023
α	298	1.030	1.493	118.0 ± 1.1	0.113 ± 0.011	6-21G**	226.4	0.093	162.6	0.095	149.6	0.131	63.8	0.002
						6-31G**	187.8	0.124	133.1	0.131	121.6	0.181	54.7	0.007
						DZP	196.0	0.122	142.3	0.130	131.2	0.176	53.7	0.008
β	298	1.020	1.520	139.1 ± 0.3	0.093 ± 0.005	6-21G**	240.9	0.093	181.3	0.078	169.6	0.116	59.6	0.015
						6-31G**	201.7	0.122	150.5	0.109	140.6	0.159	51.2	0.013
						DZP	210.9	0.121	160.4	0.111	151.1	0.156	50.5	0.010

Table 2. Calculated DQCC (χ) and asymmetry parameter (η) for α and β phases of deuterated oxalic acid dihydrate at DFT-B3LYP level of theory

Phase	T [K]	d (O_1–D_1) [Å]	d ($D_1\cdots O_3$) [Å]	χ^{EXP} [kHz]	η^{EXP}	Basis	χ^{MOL} [kHz]	η^{MOL}	χ^{CLS} [kHz]	η^{CLS}	χ^{LAT} [kHz]	η^{LAT}	χ^{DIF} [kHz]	η^{DIF}
α	15	1.045	1.447			6-21G**	208.9	0.067	149.7	0.071	138.9	0.090	59.2	0.004
						6-31G**	167.6	0.096	118.3	0.107	109.0	0.138	49.3	0.011
						DZP	174.8	0.097	125.6	0.108	116.8	0.137	49.2	0.011
α	100	1.039	1.455			6-21G**	215.4	0.066	156.4	0.067	145.6	0.085	59.0	0.001
						6-31G**	173.9	0.093	124.7	0.101	115.4	0.130	49.2	0.008
						DZP	181.6	0.094	132.6	0.102	123.8	0.129	49.0	0.008
α	298	1.030	1.493	118.0 ± 1.1	0.113 ± 0.011	6-21G**	229.3	0.068	172.8	0.060	159.9	0.086	56.5	0.008
						6-31G**	187.1	0.095	140.1	0.089	129.1	0.125	47.0	0.006
						DZP	195.8	0.096	149.1	0.091	138.7	0.125	46.7	0.005
β	298	1.020	1.520	139.1 ± 0.3	0.093 ± 0.005	6-21G**	243.2	0.069	189.3	0.046	177.7	0.072	53.9	0.023
						6-31G**	200.7	0.095	155.7	0.069	146.1	0.106	45.0	0.026
						DZP	210.3	0.095	165.6	0.073	156.7	0.108	44.7	0.022

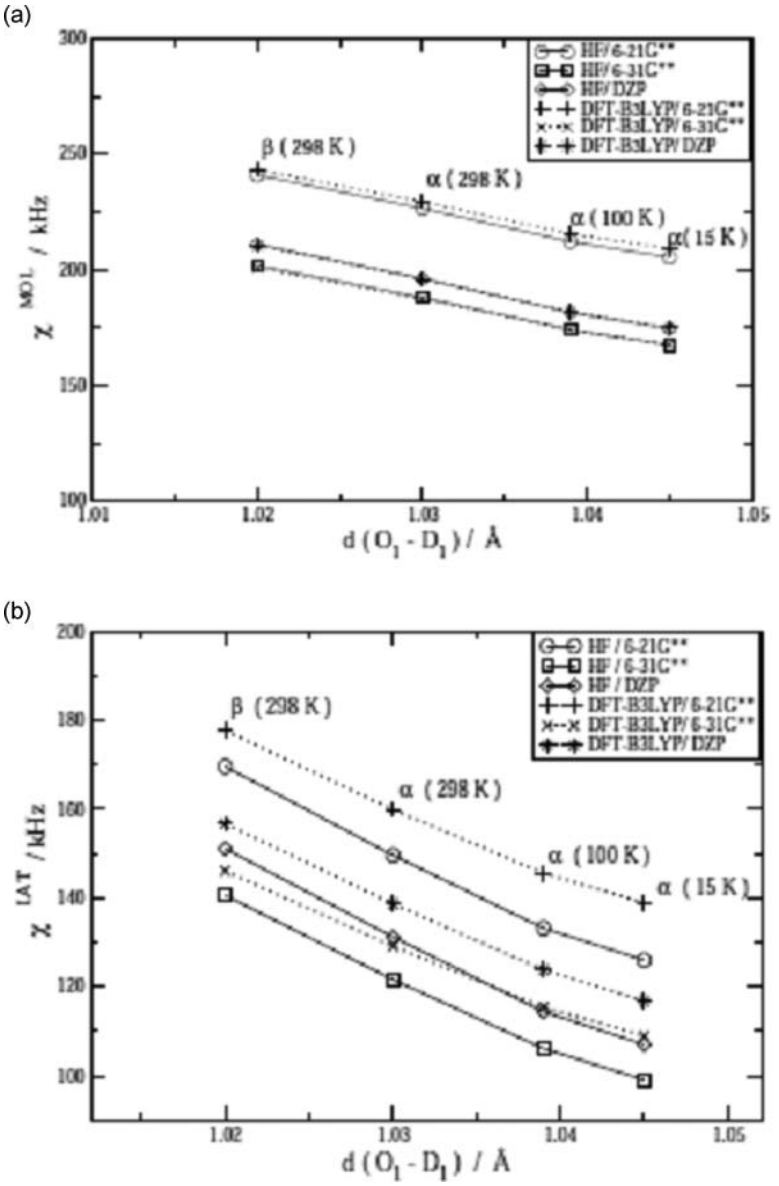

Figure 4. (a) χ^{MOL} and (b) χ^{LAT} plotted as a function of $d(O_1 - D_1)$ distance. Calculations performed at the HF and DFT-B3LYP levels of theory using the 6-21G**, 6-31G**, and DZP basis sets.

the 6-31G** basis set, as may also be observed in Figures 4(b) and 5(a). This is due to the combination of going from the HF to the DFT-B3LYP level of theory (which causes χ^{LAT} to increase) and going from the DZP to the 6-31G** basis set (which causes χ^{LAT} to decrease).

DQCCs calculated at the periodic DFT-B3LYP level of theory using 6-31G** basis set are in good agreement with experimental measurements for the crystals of oxalic acid dehydrate at 298 K, but clearly one may see that the periodic HF level of theory using the

same basis set (6-31G**) are in much better agreement with the experimental one. On the other hand, η values calculated by both the periodic HF and DFT-B3LYP approaches, using the 6-21G** basis set are equally close to the experimental measurements.

In contrast to the results presented in this study, Alfredsson et al. [5] reported that the DQCC values at DFT-B3LYP level of theory are lower for two ice polymorphs. In order to have a more clearly understanding of the effects of electronic correlation in molecular crystals, investigation on other systems displaying a range of hydrogen bonding should be carried out.

5.3 Structural Dependence

Tables 1 and 2 clearly demonstrate the structural dependence with temperature of the calculated DQCC and η values for the α phase of deuterated oxalic acid dihydrate. As the temperature decreases the DQCC values also slightly decrease; on the other hand, the η values increase by a very small value.

In particular, by lowering the temperature from 298 K to 100 K for the α phase, it can be observed that the $\chi^{MOL,}$ χ^{CLS}, and χ^{LAT} values decrease by up to 10% for the 6-21G** and by up to 12% for both the 6-31G** and the DZP basis sets. The η^{CLS} and η^{LAT} values increase by up to 2% for the 6-21G** and by about 5% for both the 6-31G** and DZP basis sets, while the η^{MOL} values practically remain unchanged. Further lowering of the temperature from 100 K to 15 K, again decreases the $\chi^{MOL,}$ χ^{CLS}, and χ^{LAT} values by up to 5% for 6-21G** and by about 6% for both the 6-31G** and DZP basis sets. The $\eta^{MOL,}$ η^{CLS}, and η^{LAT} values again increase by up to 4% for 6-21G** and by about 6% for both 6-31G** and DZP basis sets.

Temperature variation certainly produces changes in the intramolecular [$d(O_1-D_1)$] and intermolecular geometry [$d(D_1\cdots O_3)$]. From Figs. 4(a), 4(b), and 5(a) one may see how these structural variations are mirrored by changes in the χ^{LAT} and χ^{MOL} values.

Figures 4(a) and 4(b) show an early linear dependence of χ^{LAT} and χ^{MOL} on $d(O_1-D_1)$ at both the HF and the DFT-B3LYP levels of theory, and it is also interesting to notice that the χ^{LAT} and χ^{MOL} values for the β phase also fall on the same straight line for the α phase. These results also show that the χ^{LAT} values lower much more rapidly than the χ^{MOL} values on increasing $d(O_1-D_1)$ distance.

Figure 5(a) shows that the χ^{LAT} values increase linearly as $d(D_1\cdots O_3)$ increases for the α phase for both the HF and DFT-B3LYP calculations. Again the value of χ^{LAT} calculated for the β phase falls on the straight line established for the α phase.

From the results obtained from Figs. 4(b) and 5(a), it can be deduced that lowering the temperature of the α phase produces an elongation of the experimental bond length $d(O_1-D_1)$ and a shortening of the experimental hydrogen bond $d(D_1\cdots O_3)$, such that χ^{LAT} values become lower due to an electronic charge redistribution in the very close vicinity of the probed nucleus at both level of theory employed here. In contrast, for a strictly isolated oxalic acid molecule, an increase of temperature would lead to an increase in the (O_1-D_1) bond length (due to bond anharmonicity), but a corresponding decrease in DQCC values [26].

The linear relationships that we have observed above between DQCCs and the distances $d(O_1-D_1)$ and $d(D_1\cdots O_3)$, confirm the scaling and linear extrapolation previously reported by Camus et al. [26] using the 6-31G** basis set.

Temperature effects are expected to introduce some errors on geometry information, as a combination of the various dynamical processes taking place (e.g., translational, rotational, and vibrational motion). Experimental and theoretical procedures can be combined in

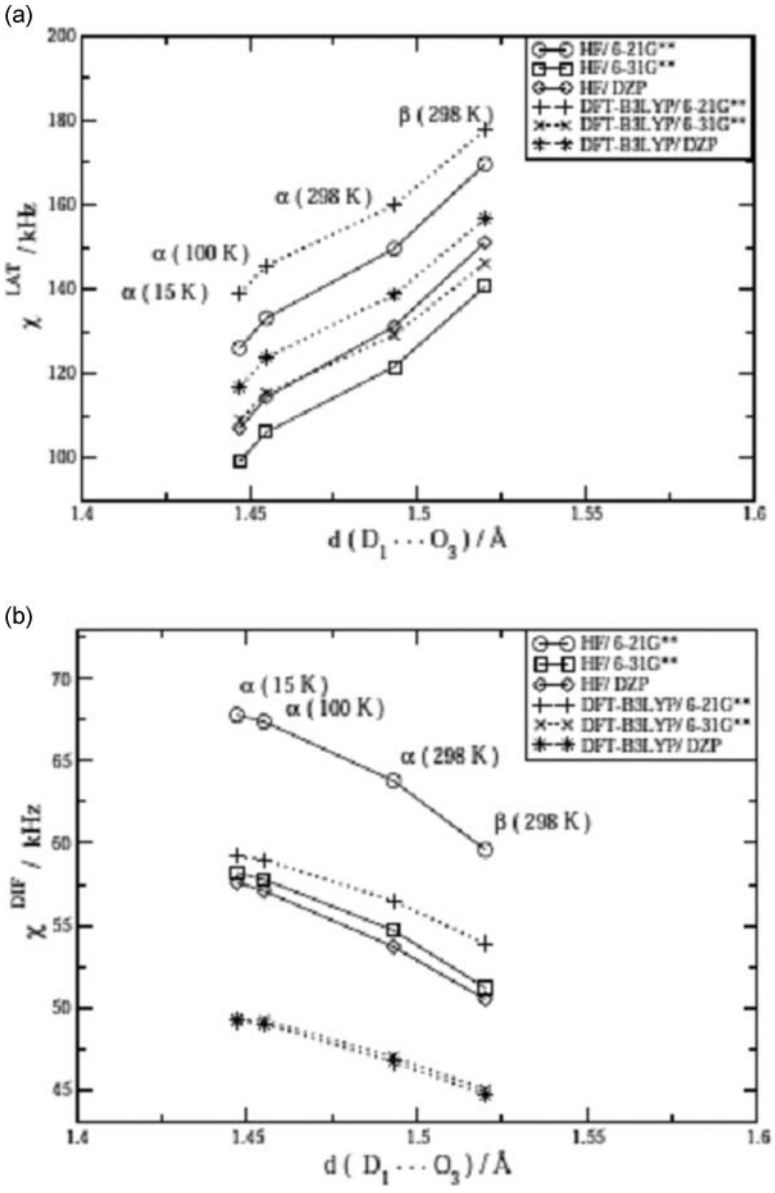

Figure 5. (a) χ^{LAT} and (b) χ^{DIF} plotted as a function of $d(D_1 \cdots O_3)$ distance. Calculations performed at the HF and DFT-B3LYP levels of theory using the 6-21G**, 6-31G**, and DZP basis sets.

order to correct such data. In particular, vibrational effects are very important for making meaningful comparison between electrical properties, which are highly sensitive to small changes in geometry and the experimentally measured properties. Generally, accurate predictions of the vibrationless property at the reference geometry are expected to be more important than obtaining extremely accurate zero-point vibration corrections (ZPVC) since the resulting basis set and correlation errors are likely to be much larger than those inferred from inaccurate ZPVCs.

5.4 Crystal Field Dependence

Tables 1 and 2 show that the χ^{LAT} values are generally smaller than the χ^{CLS} and χ^{MOL} values for both phases (α and β), independent of the level of theory (HF and DTF-B3LYP). On the other side, η^{LAT} is larger when the full periodic environment is consider rather than an isolated molecule in both α ($\eta^{LAT} > \eta^{CLS} > \eta^{MOL}$) and β ($\eta^{LAT} > \eta^{MOL} > \eta^{CLS}$) phases, however the latter clearly presents an oscillating pattern.

Introducing the four neighboring water molecules around an oxalic acid molecule reduces the DQCC such that χ^{CLS} is lower by ca. 23%–33% than $\chi^{MOL.}$ Including more distant neighbors in the periodic lattice calculation slightly decreases the DQCC by ca. 6%–8% from χ^{CLS} to χ^{LAT}. These changes imply that the main contribution to the DQCC of the periodic crystal (χ^{LAT}) arises from the intramolecular component (χ^{MOL}) in both phases.

On the other hand, the intramolecular (η^{MOL}) and intermolecular (η^{CLS}) asymmetry parameter components equally contribute to the asymmetry parameter of the periodic crystal (η^{LAT}), since introducing the four neighboring water molecules around an oxalic acid molecule increases the asymmetry parameter. It is reflected in the fact that χ^{CLS} is larger by ca. 6%–13% than χ^{MOL} for the α phase and is smaller by ca. 8%–16% than χ^{MOL} for the β phase, and also including more distant neighbors in the periodic calculation hugely increases the asymmetry parameter by 30%–48% from χ^{CLS} to χ^{LAT} for both phases.

The inclusion of electron correlation at the DFT-B3LYP level of theory qualitatively unmodifies above results and only slightly decreases the intramolecular and intermolecular contributions for both the DQCC and η values.

The effect of different crystal environments on the oxalic acid molecule is addressed by comparing the DQCCs and asymmetry parameters for the α and β phases at 298 K. One can see that χ^{MOL} presents a difference of 3 kHz between the two phases. A similar pattern is also observed for χ^{LAT}, where the difference is 10 kHz. These differences in χ^{MOL} and χ^{LAT} between both phases can be assigned to changes on the $d(O_1 - D_1)$ bond length, which imply that the main contribution is intramolecular. Additionally for χ^{LAT} minor but not less important intermolecular interactions based in more distant neighboring molecules also obviously contribute.

Figure 5(b) shows the contribution to the DQCC values from the first shell of neighboring water molecules by plotting $\chi^{DIF} = \chi^{MOL} - \chi^{CLS}$ as a function of $d(D_1 \cdots O3)$. As mentioned above, the inclusion of the first shell of water molecules results in a decrease in the value of DQCC from the isolated molecule. The effect of the first shell of water molecules becomes more important as $d(D_1 \cdots O3)$ decreases (e.g., on lowering the temperature) reflecting a stronger influence of the neighboring water molecules on the DQCC values.

6. Conclusions

Convergence problems due to basis set pseudolinear dependence previously reported by Camus et al. [26], were avoided by setting the tolerance parameters (ITOL1, ITOL2, ITOL3, ITOL4, ITOL5) at high values in order to select the Coulomb and Exchange integral symmetrically and to ensure high accuracy in their evaluation.

The DQCC and η values are very sensitive to the expansion of inner valence functions and less sensitive to the relaxation of the constraint between the exponents of the *s* and *p* valence functions.

Comparing the DQCC values calculated in this study and those obtained by Camus et al. [26], we observed that our DQCC values are generally appreciably smaller by approximately 28 kHz using the 6-21G** basis set, and slightly larger (2 kHz) using the 6-31G** basis set. Different exponent values of the 6-21G** basis set are likely explaining the significant variations on DQCC values.

The linear relationships that we have observed between DQCC (χ) values and the distances $d(O_1-D_1)$ (bond length) and $d(D_1\cdots O3)$ (the hydrogen bond distance) are in excellent agreement with those previously reported by Camus et al. [26] and validate the scaling and linear extrapolation used there.

DQCC values calculated at the periodic HF level of theory by using 6-31G** basis set are in excellent and better agreement with experimental measurements than those calculated at the DFT-B3LYP level of theory for the crystals of oxalic acid dihydrate at 298 K.

Inclusion of electron correlation the DFT-B3LYP level of theory produces slightly larger DQCC values. On the other hand, η values calculated by both the periodic HF and DFT-B3LYP approaches, using the 6-21G** basis set are equally close to the experimental measurements. For molecular crystals, where dispersion interactions are important, DFT-B3LYP augmented with an empirical dispersion term [47] and advanced periodic correlated methodologies such as Local Moller-Plesset theory (P-MP2) [48–51] should be tested in future work.

The intramolecular and intermolecular contributions to the DQCC and η have been quantified. The main contribution to DQCC arises from the intermolecular components. For η, both components contribute. Inclusion of electron correlation at the DFT-B3LYP level of theory underestimated the intramolecular and intermolecular contributions to DQCC and η values.

Performing DQCC and η calculations in the full periodic structure results into a better agreement with experimental measurements. Nonetheless, other hydrogen bonded molecular crystals should be investigated in order to test the applicability of the approaches described here.

References

[1] Dovesi, R., Causà, M., Orlando, R., Roetti, C., & Saunders, V. (1990). *J. Chem. Phys.*, *92*, 7402.
[2] Ojamae, L., Hermansson, K., Dovesi, R., Roetti, C., & Saunders, V. (1994). *J. Chem. Phys.*, *100*, 2128.
[3] Gatti, C., Saunders, V., & Roetti, C. (1994). *J. Chem. Phys.*, *101*, 10686.
[4] Silvi, B., Beltran, A., & Andres, J. (1997). *J. Mol. Struct.: Theochem.*, *437*, 443.
[5] Alfredsson, M., & Hermansson, K. (1999). *Chem. Phys.*, *242*, 161.
[6] Milanesio, M., Bianchi, R., Ugliengo, P., Roetti, C., & Viterbo, D. (1997). *J. Mol. Struct.: Theochem.*, *419*, 139.
[7] Allouche, A., Verlaque, P., & Pourcin, J. (1998). *J. Phys. Chem. B*, *102*, 89.
[8] Bussolin, G., Casassa, S., Pisani, C., & Ugliengo, P. (1998). *J. Chem. Phys.*, *108*, 9516.
[9] Spackman, M. A., Byrom, P. G., Alfredsson, M., & Hermansson, K. (1999). *Acta Cryst. A*, *55*, 30.
[10] Zavodnik, V., Stash, A., Tsirelson, V., De Vries, R., & Feil, D. (1999). *Acta Cryst. B*, *55*, 45.
[11] Cárdenas-Jirón, G. L., Masunov, A., & Dannenberg, J. J. (1999). *J. Phys. Chem. A*, *103*, 7042.
[12] Abramov, Y. A., Volkov, A. V., & Coppens, P. (1999). *Chem. Phys. Lett.*, *311*, 81.
[13] Casassa, S. (2000). *Chem. Phys. Lett.*, *321*, 1.
[14] Kulkarni, G. U., Gopalan, R. S., & Rao, C. N. R. (2000). *J. Mol. Struct.: Theochem.*, *500*, 339.
[15] Masunov, A., & Dannenber, J. (2000). *J. Phys. Chem. B*, *104*, 806.
[16] van Reewijk, S. J., van Beek, K. G., & Feil, D. (2000). *J. Phys. Chem. A*, *104*, 10901.

[17] Volkov, A., Gatti, C., Abramov, Y., & Coppens, P. (2000). *Acta Cryst. A*, *56*, 252.
[18] Zapol, P., Curtiss, L. A., & Erdemir, A. (2000). *J. Chem. Phys.*, *113*, 3338.
[19] Spackman, M. A., & Mitchell, A. S. (2001). *Phys. Chem. Chem. Phys.*, *3*, 1518.
[20] Grimwood, D. J., & Jayatilaka, D. (2001). *Acta Cryst. A*, *57*, 87.
[21] Abramov, Y. A., Volkov, A., Wu, G., & Coppens, P. (2000). *J. Phys. Chem. B*, *104*, 2183.
[22] Pyykkö, P. (1992). *Z. Naturforsch*, *47a*, 189.
[23] Pyykkö, P. (2001). *Mol. Phys.*, *99*, 1617.
[24] Lucken, E. A. C. (1969). *Nuclear Quadrupole Coupling Constants*, Academic Press: London.
[25] Brown, A. S., & Spackman, M. A. (1994). *Mol. Phys.*, *83*, 551.
[26] Camus, S., Harris, K. D., & Johnston, R. L. (1997). *Chem. Phys. Lett.*, *276*, 186.
[27] Palmer, M. H. (1990). *Z. Naturforsch*, *45a*, 357.
[28] Palmer, M. H. (1992). *Z. Naturforsch*, *47a*, 203.
[29] Palmer, M. H., & Blair-Fish, J. A. (1994). *Z. Naturforsch*, *49a*, 146.
[30] Palmer, M. H. (1996). *Z. Naturforsch*, *51a*, 442.
[31] Palmer, M. H. (1996). *Z. Naturforsch*, *51a*, 451.
[32] Palmer, M. H., & Sherwood, P. (1996). *Z. Naturforsch*, *51a*, 460.
[33] Palmer, M. H. (1996). *Z. Naturforsch*, *51a*, 479.
[34] Lehmann, A., Luger, P., Lehmann, C. W., & Ibberson, R. M. (1994). *Acta Cryst. B*, *50*, 344.
[35] Coppens, P., & Sabine, T. M. (1969). *Acta Cryst. B*, *25*, 2442.
[36] Chiba, T., & Soda, G. (1971). *Bull. Chem. Soc. Japan*, *44*, 1703.
[37] Dovesi, R., Saunders, V. R., Roetti, C., Causà, M., Harrison, N. M., Orlando, R., Zicovich-Wilson, C. M., Pascale, F., Civalleri, B., Doll, K., Harrison, N. M., Bush, I. J., 'Arco, P. D., & Llunell, M. (2009). *CRYSTAL09 User's Manual*, University of Torino: Torino.
[38] Becke, A. D. (1993). *J. Chem. Phys.*, *98*, 5648.
[39] Lee, C., Yang, W., & Parr, R. G. (1988). *Phys. Rev. B*, *37*, 785.
[40] Binkley, J. S., Pople, J. A., & Hehre, W. J. (1980). *J. Am. Chem. Soc.*, *102*, 939.
[41] Hehre, W. J., Ditchfield, R., & Pople, J. A. (1972). *J. Chem. Phys.*, *56*, 2257.
[42] Hehre, W. J., & Pople, J. A. (1972). *J. Chem. Phys.*, *56*, 4233.
[43] Dill, J. D., & Pople, J. A. (1975). *J. Chem. Phys.*, *62*, 2921.
[44] Thakkar, A. J., Koga, T., Saito, M., & Hoffmeyer, R. E. (1993). *Int. J. Quantum Chem.*, *27*, 343.
[45] Hariharan, P. C., & Pople, J. A. (1973). *Theor. Chim. Acta*, *28*, 213.
[46] Becke, A. D. (1988). *J. Chem. Phys.*, *88*, 2547.
[47] Civalleri, B., Zicovich-Wilson, C., Valenzano, L., & Ugliengo, P. (2008). *Cryst. Eng. Comm.*, *10*, 405.
[48] Pisani, C., Maschio, L., Casassa, S., Halo, M., Schütz, M., & Usvyat, D. (2008). *J. Comp. Chem.*, *29*, 2113.
[49] Erba, A., Casassa, S., Maschio, L., & Pisani, C. (2009). *J. Phys. Chem. B*, *113*, 2347.
[50] Erba, A., Pisani, C., Casassa, S., Maschio, L., Schütz, M., & Usvyat, D. (2010). *Phys. Rev. B*, *81*, 165108.
[51] Maschio, L., Usvyat, D., & Civalleri, B. (2010). *Cryst. Eng. Comm.*, *12*, 2429.